Defence Science Journal, Vol. 60, No. 3, May 2010, pp. 233-237

Parametric Analysis of Energy Absorption in Micro-particle Photophoresis in Absorbing Gaseous Media

W.K. Li, C.Y. Soong, C.H. Liu**, and P.Y. Tzeng#

Chung Cheng Institute of Technology, National Defense University, Tahsi, Taoyuan 33509, Taiwan, ROC
E-mail:g990401@ccit.edu.tw, #E-mail:pytzeng@ccit.edu.tw
**Feng Chia University, Seatwen, Taichung 40724, Taiwan, ROC*
E-mail:cysoong@fcu.edu.tw
***Yuanpei University, Hsinchu 30015, Taiwan, ROC*
E-mail: chungho@mail.ypu.edu.tw

ABSTRACT

The study deals with photophoresis of a spherical micro-particle suspended in absorbing gaseous media. Photophoretic motion of the particle stems from the asymmetric distribution of absorbed energy within the particle. By evaluating the so-called heat source function at various conditions, the study focuses on the effects of governing parameters on the energy distribution within the particle and their potential influences to the photophoresis. The results reveal that the increase in either particle size or absorptivity enhances the energy intensity on the illuminated (leading) side and tends to generate positive photophoresis. For a particle of low absorptivity, the energy distribution is dominated by particle refraction. Enhancing particle refractivity, the energy tends to be focused onto a certain spot area on the shaded (trailing) side and leads to a tendency of negative photophoresis. Increasing medium absorptivity significantly degrades the level of energy absorbed by the particle and in turn weakens the driving force of the particle photophoresis.

Keywords: Heat source function, size parameter, absorptivity, refractivity, particle photophoresis

NOMENCLATURE

c	Speed of light in vacuum
c_n, d_n	Internal electric field coefficients
E	Electric field amplitude vector
E_0	Amplitude of incident electric field
H	Amplitude vector of magnetic field
i	Indication for imaginary part
k	Thermal conductivity
m	Complex refractive index
n	Real part of refractive index
P_n	Legendre polynomial
Q	Radiant-absorption heat source function
r	Radial coordinate
R	Particle radius
T	Temperature

Greek symbols

α	Particle size parameter
θ	Polar coordinate
κ	Imaginary part of refractive index
λ	Wavelength
λ_0	Wavelength in vacuum
μ	Magnetic permeability
ξ_n	Hankel function
ϕ	Azimuthal coordinate
χ_n	Second kind Ricatti-Bessel function
ψ_n	First kind Ricatti-Bessel function
σ	Particle electrical conductivity

Superscripts

*	Complex conjugate
'	Differentiation wrt argument

Subscripts

a	Ambient
p	Particle
n	Index
r, θ, ϕ	Spherical coordinate system components

1. INTRODUCTION

Aerosol particles in atmosphere may affect the light direction and the air visibility through absorbing and scattering light. With the feature of visibility degradation due to the presence of the suspended particles, a smoke screen in defence can be employed to mask the movement or location of military units. A suspended aerosol particle encounters gravity, buoyancy, and frictional drag. Some particles could be caused to levitate and others induced to fall more rapidly[1]. It was shown that the altitude at which the photophoretic force balancing gravity

Received 28 March 2009, Revised 25 August 2009

corresponds to the altitude where observed aerosol layer existing in the atmosphere[2]. It may be considered as an evidence for a possible role of photophoretic forces in aerosol stratification in the atmosphere[3]. In previous experimental studies, it has been shown that the effect of sunlight on aerosol behaviour in the atmosphere could be significant and sometimes even stronger than the gravitational influence on individual aerosol particles[4]. Atmospheric aerosols also significantly influence climate of the earth and human health[5]. Besides the military applications, this class of optofluidic mechanisms also have applications in other engineering disciplines.

In optical radiation fields, it has been well-known that a particle subjected to an intense light beam absorbs and scatters light and turns electromagnetic energy into thermal energy within the particle. The uneven heat distribution in the particle will cause the photophoresis force, which might drives the particle either toward (negative photophoresis) or away from (positive photophoresis) the light source. The photophoretic force stems from the internal energy absorbed by the particle, for which the so-called heat source function (HSF) within the particle is a key. A number of works have been devoted towards the calculation of HSF based on the Mie scattering theory in non-absorbing media[6-10]. But in general, the medium surrounding the particles may contain constituents with significant absorption. For example, ozone and CO_2 in the atmosphere have strong absorptive bands at 9.6 μm and 15 μm, respectively[11]. The effects of the medium absorptivity on HSF of a particle is important to many applications including light scattering by cloud particles surrounded, water vapours in the atmosphere, biological particles in the ocean, and air bubbles in the ocean and sea ice[12]. For an absorbing medium, the Mie theory is no longer valid and the Mie equations have to be modified. A few studies have been carried out to develop the theoretical models and the properties of light scattering by spherical[13-17] and non-spherical[18-21] particles suspended in the absorbing medium.

From the above review of previous studies of micro-particle photophoresis, it is found that the effects of optical properties of particle and gaseous medium on the radiants absorption were not investigated in details, especially in the case of absorbing medium. The present work performs a detailed parametric analysis for the photophoresis of an absorbing particle in absorbing gaseous medium. Variations of the absorbed energy by the micro-particle at various conditions have been evaluated. The underlying physical mechanisms have also been addressed.

2. THEORETICAL BACKGROUND

As shown in Fig. 1, an isotropic homogenous particle is suspended in a gaseous fluid with a monochromatic, parallel, and linearly polarised light beam along the z-direction. The temperature distribution in the particle, T_p, is described by the solution to the following equation:

$$\nabla^2 T_p = -\frac{Q(r,\theta)}{k_p} \tag{1}$$

where, k_p is the thermal conductivity of the particle, and $Q(r,\theta)$ is the radiant absorption which can be related to Poynting vector and is given[6] by

$$Q(r,\theta) = -Re\nabla\left[\frac{1}{2}\left(E\times H\right)\right] = \frac{1}{2}\sigma E\bullet E^* \tag{2}$$

In the above equation, σ is the electrical conductivity of the particle, and

$$\sigma = \frac{4\pi n_p \kappa_p}{\lambda_0 \mu c} \tag{3}$$

where, n_p and κ_p are the real and imaginary parts of the complex refractive index of a particle, $m_p = n_p + \kappa_p i$, λ_0 is the wavelength in vacuum, μ the magnetic permeability, and c the speed of light in vacuum.

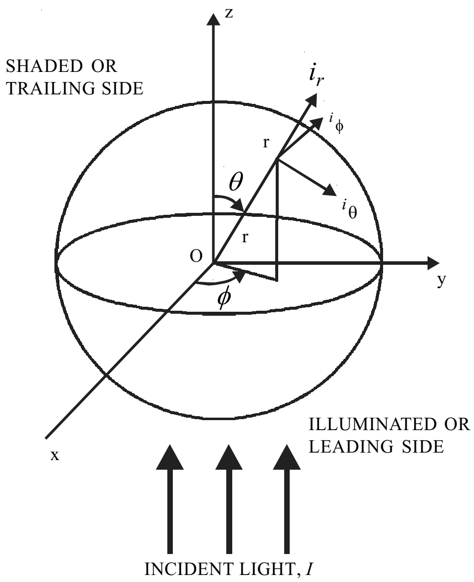

Figure 1. Physical model of a microspherical particle photophoresis.

The HSF can be characterised by the magnitude of $|\mathbf{E}|^2$, for which there is a need to evaluate the components of the internal electric field within the particle, i.e., E_r, E_θ, and E_ϕ, which can be expressed[22,23] as:

$$E_r = -\frac{E_0\cos\phi}{m^2\alpha^2}\sum_{n=1}^{\infty} i^{n+1}\left(2n+1\right)d_n P_n^{(1)}\left(\cos\theta\right)\psi_n\left(m\alpha\right) \tag{4}$$

$$E_\theta = \frac{E_0\cos\phi}{m\alpha}\sum_{n=1}^{\infty}\frac{i^n\,2n+1}{n\left(n+1\right)}\left[c_n\psi_n\left(m\alpha\right)\frac{P_n^{(1)}\left(\cos\theta\right)}{\sin\theta} - id_n\psi_n'\left(m\alpha\right)P_n^{(1)\prime}\left(\cos\theta\right)\sin\theta\right] \tag{5}$$

$$E_\phi = -\frac{E_0\sin\phi}{m\alpha}\sum_{n=1}^{\infty}\frac{i^n\,2n+1}{n\left(n+1\right)}\left[c_n\psi_n\left(m\alpha\right)P_n^{(1)\prime}\left(\cos\theta\right)\sin\theta - id_n\psi_n'\left(m\alpha\right)\frac{P_n^{(1)}\left(\cos\theta\right)}{\sin\theta}\right] \tag{6}$$

The coefficients c_n and d_n in the above equations for Mie scattering in absorbing media are given[17] by:

$$c_n = \frac{m_p\xi_n\left(m_a\alpha\right)\psi_n'\left(m_a\alpha\right) - m_p\xi_n'\left(m_a\alpha\right)\psi_n\left(m_a\alpha\right)}{m_p\xi_n\left(m_a\alpha\right)\psi_n'\left(m_p\alpha\right) - m_a\xi_n'\left(m_a\alpha\right)\psi_n\left(m_p\alpha\right)} \tag{7}$$

$$d_n = \frac{m_p\xi_n\left(m_a\alpha\right)\psi_n'\left(m_a\alpha\right) - m_p\xi_n'\left(m_a\alpha\right)\psi_n\left(m_a\alpha\right)}{m_a\xi_n\left(m_a\alpha\right)\psi_n'\left(m_p\alpha\right) - m_p\xi_n'\left(m_a\alpha\right)\psi_n\left(m_p\alpha\right)} \tag{8}$$

where E_0 is the amplitude of incident electric field, m is the refractive index of the spherical particle relative to the gaseous medium, $\alpha \equiv 2\pi R/\lambda$ is the size parameter, $\xi_n = \psi_n + i\chi_n$ is the Hankel function, and ψ_n and χ_n denote the Ricatti-Bessel functions of the first kind and second kind, respectively.

3. RESULTS AND DISSCUSSION

For an absorbing medium, the incident electric field amplitude, $E_0 = \exp(-\kappa_a \alpha)$, used in a number of previous studies[13,14,23] is adopted. The present calculation of HSF distribution within a particle in absorbing media has been successfully verified as comparing with the previous results[14].

3.1 Effects of Particle Size

The absorbing abilities of particles and gases depend on the wavelength of the incident light. For example, carbon dioxide, water, and ozone may absorb energy at wavelengths between 4 μm and 26 μm[24]. In this situation, the absorption coefficients of the particles have the values of 0.135–0.290 for dust, 0.051–0.325 for quartz, 0.732 for acetylene soot[25], etc.

With consideration of the above-mentioned data, the values of κ_p from 0.06 to 0.4 are adopted in the present analysis. As to the absorption coefficient of air, κ_a, values up to 0.5 were used in previous studies[12,14]. Here, the values of κ_a from 0 to 0.2 are considered.

Figure 2 presents the HSF distributions with changes in particle size parameter at the condition of m_a=1.0+0.01i and m_p=1.5+0.06i. In the case of α=0.5 shown in Fig. 2(a), the internal energy distribution with such a small size is nearly uniform. For a larger particle size, α=10 in Fig. 2(b), the particle acts as a microlens and the incident light or energy is absorbed and focused in a region close to the shaded (trailing) surface. This situation may lead to a negative photophoresis. At α=20, the distance of light path within the particle is longer and the illuminated (leading) surface absorbs more energy from the incident light yielding a symmetrical distribution as shown in Fig. 2(c). As the particle size further increases to α=40, Fig. 2(d) shows that the HSF peak near the trailing side diminishes and the energy absorbed by the leading surface becomes dominant, which is beneficial to the occurrence of positive photophoresis.

3.2 Effects of Particle Refractivity

To highlight the influences of light refraction, both small absorptivities of particle and gas medium, i.e., κ_p = 0.06 and κ_a = 0.01, are used in analysis. For the micro-particle of size α=10 and refractivity n_p = 1.1, since the incident light is difficult to focus in the interior region of the particle, the HSF is nearly uniform and of low level as shown in Fig. 3(a). When the particle refraction increases to n_p = 2.0, a highlighted region of the HSF appears near the shaded (trailing) side, which leads to a negative photophoresis in Fig. 3(b). Enhancing the particle refraction to n_p = 3.0, (Fig. 3(c)), the absorption peak becomes more evident and moves gradually forward. Finally, at n_p = 4.0, the refraction generates a sharp absorption peak and moves towards the particle centre (Fig. 3(d)). From the above HSF contours, it is obvious that the variation in light refraction is the major reason for the movement of the energy spot location. The light refracted by the micro particle focuses onto a certain spot area located between the center and the trailing surface of the particle, and the limit of the forward movement is the particle centre. The wave-like pattern of HSF contours in Fig. 3(d) comes from the continuous reflection of the internally refracted rays within the particle.

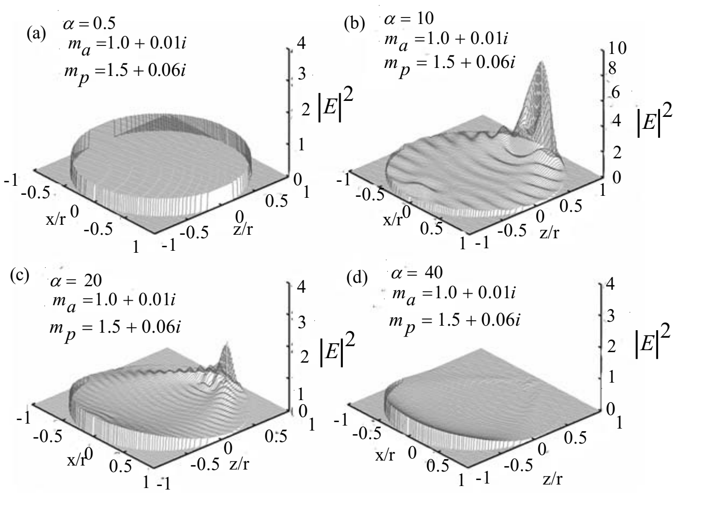

Figure 2. Heat source function in an absorbing gas medium of m_a =1.0 + 0.01i for an absorbing spherical particle of m_p =1.5 + 0.06i. The values of the particle size parameter are: (a) α = 0.5; (b) α = 10; (c) α = 20; and (d) α = 40.

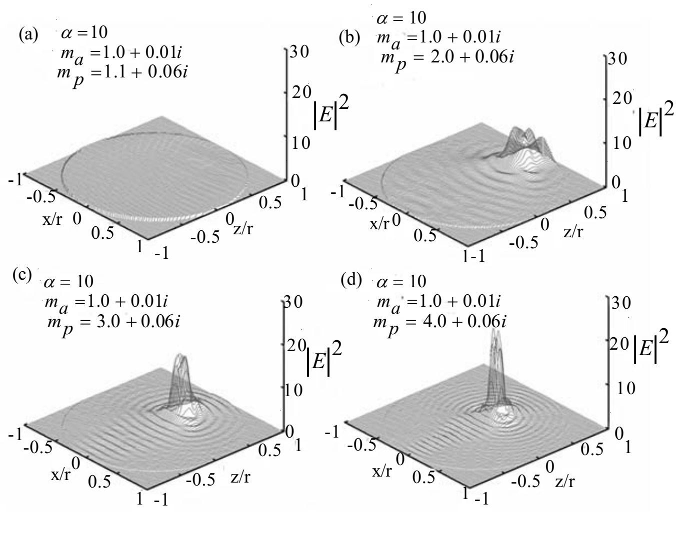

Figure 3. Effects of particle refractivity on the heat source function in an absorbing gas medium of m_a =1.0 + 0.01i for a weakly absorbing particle of m_p = n_p+0.06i and α= 10 with: (a) n_p = 1.1; (b) n_p = 2.0; (c) n_p = 3.0; and (d) n_p = 4.0.

3.3 Effects of Particle Absorptivity

Figure 4 presents the effect of particle absorptivity κ_p on the HSF distribution within a particle of $\alpha=10$ and low refractivity $n_p = 1.5$ in an absorbing medium of $m_a=1.0 + 0.01i$. At the low aborptivity, $\kappa_p = 0.06$, the particle exerts strong microlens effect and a salient HSF peak lies close to the trailing surface (Fig. 4(a)). As the particle absorptivity increases to $\kappa_p = 0.1$ (Fig. 4(b)), more energy of the incident light is absorbed by the illuminated leading surface and the HSF peak located near the trailing surface of the particle is obviously weakened. An increase in the particle absorptivity, $\kappa_p = 0.2$, enhances light absorption of the illuminated surface and enables premature positive photophoresis in Fig. 4(c). At further higher absorptivities, $\kappa_p = 0.4$, the HSF distribution shown in Fig. 4(d) demonstrates the energy absorbed by the leading surface and the HSF peak diminished noticeably.

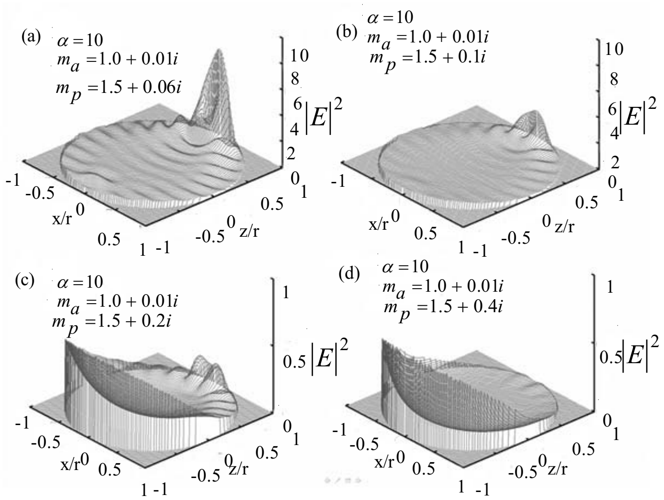

Figure 4. Effects of particle absorptivity on the heat source function in an absorbing gas medium of m_a =1.0 + 0.01*i* for a low refractive particle of m_p=1.5 + κ_p*i* and α = 10 with (a) κ_p = 0.06; (b) κ_p = 0.1; (c) κ_p = 0.2; and (d) κ_p = 0.4.

3.4 Effects of Gas Medium Absorptivity

Figure 5 reveals the effects of the gaseous medium absorptivity on HSF distribution, in which the results for particles of size $\alpha=10$, $m_p=1.5+0.1i$, and $m_a=1.0+\kappa_a i$ with $\kappa_a = 0.0$, 0.05, 0.1, and 0.2 are presented. In non-absorbing medium, $\kappa_a = 0.0$, the absorption centre locates on the trailing side of the particle (Fig. 5(a)). With increasing light absorption of the medium, part of the incident energy is absorbed by the medium. Therefore, both the energy reaching at the particle and also the energy focused onto the area near the trailing surface are reduced. As a result, the HSF peak and the energy level within the particle are both decreased as shown in Figs 5(b) and 5(c). In Fig. 5(d) for $\kappa_a = 0.2$, more energy is absorbed by the medium, and the intensity of the peak on the trailing side diminishes.

4. CONCLUSIONS

In the present work, a parametric analysis of energy absorption concerned with photophoresis of a micro-particle in absorbing gaseous medium has been performed. The results demonstrate that the energy distribution inside the micro- particle is highly dependent of the particle size and optical properties of the particle and the background medium. Based on the present analysis, the following conclusions can be drawn:

The increase in either particle size or absorptivity enhances the energy intensity on illuminated or leading side and tends to generate positive photophoresis. For a particle of low absorptivity, the energy distribution is dominated by particle refraction. Enhancing the refractivity, the energy from the incident light tends to be focused onto a certain spot area on the shaded (trailing) side and thus leads to a tendency of negative photophoresis. Moreover, increasing medium absorptivity significantly degrades the level of energy absorbed by the particle, which will in turn weaken the driving force of the particle photophoresis.

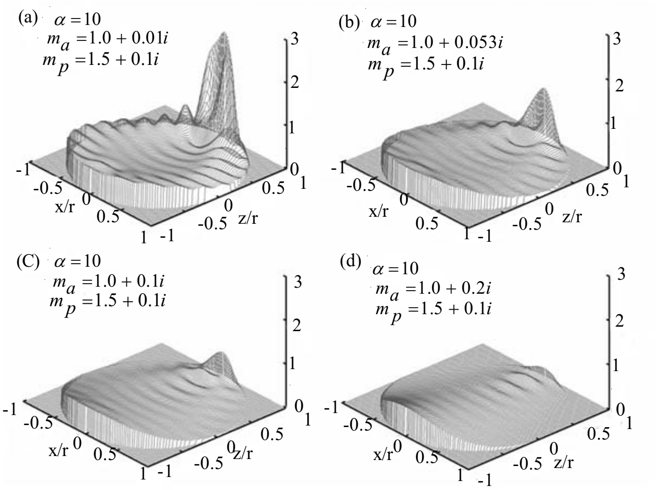

Figure 5. Effects of medium absorptivity on the heat source function for a low refractive particle of m_p =1.5+0.1*i* and α= 10 in gas media of m_a =1.0 + κ_ai with (a) κ_a= 0; (b) κ_a =0.05; (c) κ_a = 0.1; and (d) κ_a = 0.2.

ACKNOWLEDGMENTS

This study was supported by National Science Council of the Republic of China (Taiwan) through the Grant NSC96-2221-E-264-002. The first author would like to gratefully acknowledge Dr I.W. Sudiarta for his useful discussion.

REFERENCES

1. Kerker, M. & Cooke, D.D. Photophoretic force on aerosol particles in the free molecule regime. *J. Opt. Soc. Amer.*, 1982, **72**, 1267-272.
2. Cheremisin, A.A.; Vassilyev, Yu,V. & Kushnarenko, A.V. Photophoretic forces for bispherical aerosol particles. *SPIE Proceedings*, 2002, **5027**, 23-34.
3. Cheremisin, A.A.; Vassilyev, Yu,V. & Horvath, H. Gravito-photophoresis and aerosol stratification in the atmosphere. *J. Aerosol Sci.*, 2005, **36**, 1277-299.
4. Reed, L.D. Low Knudsen number photophoresis. *J. Aerosol Sci.*, 1977, **8**, 123-31.
5. Haisch, C.; Kykal, C. & Niessner, R. Photophoretic

velocimetry for the characterization of aerosols. *Analytical Chemistry*, 2008, **80**, 1546-551.
6. Dusel, P.W.; Kerker, M. & Cooke, D.D. Distribution of absorption centers within irradiated spheres. *J. Opt. Soc. Amer.*, 1979, **69**, 55-59.
7. Pluchino, A.B. Photophoretic force on particles for low knudsen number. *Applied Optics*, 1983, **22**, 103-06.
8. Greene, W.M.; Spjut, R.E.; Bar-Ziv, E.; Sarofim, A.F. & Longwell, J.P. Photophoresis of irradiated spheres: absorption centers. *J. Opt. Soc. Amer. B*, 1985, **2**, 998-004.
9. Dobson, C.C. & Lewis, J.W.L. Survey of the Mie problem source function. *J. Opt. Soc. Amer. A.*, 1989, **6**, 463-66.
10. Tehranian, S.; Giovane, F.; Blum, J.; Xu, Y. L. & Gustafson, B.A.S., Photophoresis of micrometer-sized particles in the free-molecular regime. *Int. J. Heat Mass Transf.*, 2001, **44**, 1649-657.
11. Yang, P.; Gao, B.C.; Wiscombe, W.J.; Mishchenko, M.I.; Platnick, S.E.; Huang, H.L.; Baum, B.A.; Hu, Y.X.; Winker, D.M.; Tsay, S.C.; & Park, S. K. Inherent and apparent scattering properties of coated or uncoated spheres embedded in an absorbing host medium. *Applied Optics*, 2002, **41**, 2740-759.
12. Fu, Q. & Sun, W. Mie theory for light scattering by a spherical particle in an absorbing medium. *Applied Optics*, 2001, **40**, 1354-361.
13. Mundy, W.C.; Roux, J.A. & Smith, A.M. Mie scattering by spheres in an absorbing medium. *J. Opt. Soc. Amer.*, 1974, **64**,1593-597.
14. Sudiarta, I.W. & Chylek, P. Mie-scattering formalism for spherical particles embedded in an absorbing medium, *J. Opt. Soc. Amer. A.*, 2001, **8**, 1275-78.
15. Sudiarta, I.W. & Chylek, P., Mie scattering efficiency of a large spherical particle embedded in an absorbing medium. *J. Quant. Spectrosc. Radiat. Transf.*, 2001, **70**, 709-14.
16. Sharmaa, S.K. & Jonesb, A.R. Absorption and scattering of electromagnetic radiation by a large absorbing sphere with highly absorbing spherical inclusions. *J. Quant. Spectrosc. Radiat. Transf.*, 2003, **79**, 1051-60.
17. Fu, Q. & Sun, W. Apparent optical properties of spherical particles in absorbing medium. *J. Quant. Spectrosc. Radiat. Transf.*, 2006, **100**,137-42.
18. Ruppin, R. Extinction by a circular cylinder in an absorbing medium. *Optical Communication*, 2001, **211**, 335-40.
19. Sun, W.; Loeb, N.G. & Lin, B. Light scattering by an infinite circular cylinder immersed in an absorbing medium. *Applied Optics*, 2005, **44**, 2338-42.
20. Mishchenko, M.I. Electromagnetic scattering by a fixed finite object embedded in an absorbing medium. *Optical Express*, 2007, **15**, 13188-202.
21. Mishchenko, M.I. Multiple scattering by particles embedded in an absorbing medium. 1. Foldy–Lax equations, order-of-scattering expansion, and coherent field. *Optical Express*, 2008, **16**, 2288-301.
22. Kerker, M. The scattering of light and other electromagnetic radiation. Academic Press, New York, 1969. 666 p.
23. Bohren, C. F. & Huffman, D.R. Absorption and scattering of light by small particles. Wiley-Interscience, New York, 1983. 530 p.
24. McNab, B.K. The physiological ecology of vertebrates: A view from energetics. Cornell University Press, New York, 2002. 576 p.
25. Schleusener, S.A.; Lindberg, J.D.; White, K.O. & Johnson, R.L. Spectrophone measurements of infrared laser energy absorption by atmospheric dust. *Applied Optics*, 1976, **15**, 2546-550.

Contributors

Mr Wen-Ken Li received his Masters Degree from Chung-Cheng Institute of Technology, National Defense University, Taiwan, ROC, in 2003. He is a PhD student at Chung-Cheng Institute of Technology, National Defense University. He has worked on light scattering, optofluidics, multi-physics interfacial phenomena, etc.

Dr Chyi-Yeou Soong received his Doctoral Degree (Power Mechanical Engineering) from National Tsing Hua University, Taiwan, ROC, in 1991. Currently, he is FCU Distinguished Professor affiliated to the Department of Aerospace and Systems Engineering. His research areas include: Transport and interfacial phenomena in micro/nanofluidics, optofluidics, transport phenomena in energy systems, nonlinear dynamics and chaos control, unmanned micro/mini air vehicles, bio-flapping flight, thermofluids in rotating systems, etc.

Dr Chung-Ho Liu received his Doctoral Degree (Aeronautical Engineering) from Imperial College, UK, in 1995. Currently, he is the Dean of the College of Biomedical Science and Technology. His research areas include: haemodynamic simulation of aneurysm coiling, transport phenomena in microfluidics, optofluidics, numerical simulation of annual reverse-flow gas turbine combustor, transport phenomena in wind energy systems, and vortex method and its applications.

Dr Pei-Yuan Tzeng received his Masters Degree (Aeronautics and Astronautics) from Stanford University and PhD (Aerospace Engineering) from the University of Michigan, in 1977 and 1985 respectively. Currently, he is Professor affiliated to the Department of Mechatronic, Energy and Aerospace Engineering, National Defense University, Taiwan, ROC. His research areas include: DSMC modelling of rarefied gas flow and heat transfer in micro/nano systems, optofluidics, computational gas dynamics in propulsion systems, turbulence modelling, etc.